Renal Angiomyolipoma Based on New Classification: How to Differentiate It From Renal Cell Carcinoma

Byung Kwan Park[1]

OBJECTIVE. The purpose of this article is to describe useful imaging features for differentiating angiomyolipoma (AML) subtypes from renal cell carcinoma subtypes.

CONCLUSION. A newer radiologic classification of renal AML consists of fat-rich AML (≤ –10 HU), fat-poor AML (> –10 HU; tumor-to-spleen ratio < 0.71; signal intensity index, > 16.5%), and fat-invisible AML (> –10 HU; tumor-to-spleen ratio, > 0.71; signal intensity index, < 16.5%). Each subtype must be differentiated from the renal cell carcinoma subtype because of overlapping imaging features.

Song et al. [1] reported on a new radiologic classification of renal angiomyolipoma (AML) in which they classified the tumor into three subtypes: fat-rich AML, fat-poor AML, and fat-invisible AML. Each AML subtype is defined according to the amount of fat, which is quantified with CT or MRI [1, 2]. Fat-rich AML measures –10 HU or less at CT [1, 2]. Both fat-poor AML and fat-invisible AML measure more than –10 HU. Fat-poor AML has a tumor-to-spleen ratio less than 0.71 or signal intensity index greater than 16.5% [1, 2]. Fat-invisible AML is defined as a tumor-to-spleen ratio of 0.71 or greater and a signal intensity index of 16.5% or less [1, 2]. The Song classification [1] is simpler and more imaging based than the Jinzaki classification [3], which is complex and based on pathologic and clinical data [2].

The imaging features of renal cell carcinoma (RCC) overlap those of AML. Therefore, radiologists need to know which imaging findings are useful in discriminating AML from RCC. They may have questions about which RCC subtype is necessary for differentiating the RCC from AML subtypes. The Song classification also requires detailed explanations for radiologists to actively aid them in practice. This new classification has been introduced into practice, but it is not widely used because radiologists are not familiar with how to apply it. The purpose of this review is to show how to differentiate AML subtypes of the Song classification from RCC subtypes.

Fat-Rich Angiomyolipoma Versus Fat-Containing Renal Cell Carcinoma

Fat-rich AML is defined as a lesion measuring –10 HU or less on unenhanced CT images [1, 2, 4] (Table 1 and Fig. 1). This subtype constitutes approximately 95% of renal AMLs [5]. Almost all fat-rich AMLs are easily diagnosed with unenhanced CT alone because fat, a hallmark of AML, is clearly visualized [1–3] (Fig. 1). However, a very small number of RCCs can also contain fat [6–13] (Fig. 2). Therefore, fat-rich AML should be differentiated from fat-containing RCC even if this situation is extremely rare in clinical practice. Radiologists need to know how to differentiate fat-rich AML and fat-containing RCC because they are managed differently. Fat-rich AML requires observation, but fat-containing RCC requires surgery.

The imaging features of fat-containing RCC are not well known because only a few case reports have been published [6–13]. The size range of fat-containing RCCs is 2.7–13 cm. The median size is 9.3 cm [6–14], however, making 2.7 cm an unusual size for fat-containing RCC. Interestingly, the amounts of fat are small compared with the size of RCC [6–10, 12, 13] (Fig. 2). The median fat size was often estimated at less than 1 cm in the figures in the case reports [6–10, 12, 13]. Therefore, large tumor size with a small amount of fat is a characteristic finding suggesting fat-containing RCC. However, comparing the sizes of fat-containing RCC and fat-rich AML requires more validation. Further investigation is

Keywords: angiomyolipoma, kidney, MDCT, MRI, renal cell carcinoma

doi.org/10.2214/AJR.18.20408

Received July 20, 2018; accepted after revision September 23, 2018.

[1]Department of Radiology, Samsung Medical Center, Sungkyunkwan University School of Medicine, 50 Ilwon-dong, Kangnam-ku, Seoul, 135-710, Republic of Korea. Address correspondence to B. K. Park (rapark@skku.edu; 1436park@gmail.com).

AJR 2019; 212:582–588

0361–803X/19/2123–582

TABLE 1: Song Classification

Subtype	Diagnostic Criteria		Differential Diagnosis	Necessity of Biopsy
	Unenhanced CT	Chemical-Shift MRI		
Fat rich	≤ –10 HU	NA	Fat-containing RCC	No, but yes in exceptional cases
Fat poor	> –10	Tumor-to-spleen ratio < 0.71 or signal intensity index > 16.5%	Clear cell RCC	Controversial
Fat invisible	> –10 HU	Tumor-to-spleen ratio ≥ 0.71 and signal intensity index ≤ 16.5%	Non–clear cell RCC	Yes

Note—NA = not applicable, RCC = renal cell carcinoma.

also necessary to compare the amounts of fat in RCC and AML.

Calcification [6, 11, 12, 14] or necrosis [9, 12, 13] can be detected with CT or MRI (Fig. 2). Percutaneous biopsy is not necessary for fat-rich AML [1, 2]. However, if a renal mass contains calcification or necrosis in addition to a small amount of fat, image-guided biopsy should be recommended to exclude the likelihood of RCC [15]. Histologically, these RCCs have the characteristics of bone metaplasia containing fat foci [6, 10, 11]. Even if this metaplasia is histologically detected, calcification may not be detected with CT [10]. The non–clear cell type [6, 7, 9, 12, 13] is more common than the clear cell type [8, 10, 11] among the fat-containing RCCs (Fig. 2). When a renal mass with a fairly small amount of fat is detected, calcification or necrosis is a useful imaging feature to discriminate fat-rich AML and fat-containing RCC. Several case reports [7, 8, 10] showed that small fat foci alone can be scattered within a large RCC. This imaging feature may suggest fat-containing RCC, but further investigation is necessary to validate that it is a useful sign of RCC.

Fat-Poor Angiomyolipoma Versus Clear Cell Renal Cell Carcinoma

Approximately 5% of renal AMLs histologically have a small amount of fat [5] and correspond to fat-poor AML or fat-invisible AML in the Song classification. Among small (< 4 cm) renal tumors, 4–13% are histologically confirmed as AML because imaging shows too little fat [16–18]. Many authors [18–21] have shown that AML with a small amount of fat is likely to have female predominance, small size, and a more homogeneous texture than RCC. RCC tends to be more heterogeneous because of necrosis, calcification, or hemorrhage.

Fat-poor AML is defined as a lesion measuring more than –10 HU on unenhanced CT images but having a tumor-to-spleen ratio less than 0.71 or a signal intensity index greater than 16.5% on chemical-shift MR images [1] (Table 1 and Fig. 3). However, many clear cell RCCs also have a tumor-to-spleen ratio less than 0.71 or a signal intensity index greater than 16.5% because of abundant intracytoplasmic lipid [19–24] (Fig. 4). It is rare that non–clear cell RCC has these MRI characteristics because it contains little intracytoplasmic lipid [20, 24]. Therefore, fat-poor AML must be differentiated from clear cell RCC. This situation is common in practice because clear cell RCC is the most common subtype [25].

Qualitative analysis is frequently more useful for lesion differentiation. A decrease in signal intensity in fat-poor AML is more discrete and focal than that in clear cell RCC on opposed-phase MR images [1, 2, 20] (Table 2 and Figs. 3 and 4). Clear cell RCC tends to exhibit a diffuse decrease in signal intensity, which is less discrete than in fat-poor AML [1, 2, 20]. However, further investigation is necessary to validate these different imaging features of fat-poor AML and clear cell RCC.

Outwater et al. [23] reported that the decrease in signal intensity of some RCCs is focal. However, the clear cell RCCs in their study were quite large. They did not provide tumor sizes, but in their figures, the RCCs with signal-intensity decrease appeared larger than 3 cm. Jeong et al. [20], Song et al. [1], and Park [2], however, analyzed small renal masses (mostly smaller than 3 cm) with CT and MRI. They reported that the signal-intensity decrease in fat-poor AML is more discrete and focal than that in clear cell RCC on opposed-phase MR images and that clear cell RCC tends to exhibit a diffuse decrease in signal intensity that is less discrete than that in fat-poor AML. Further investigation is necessary because only a small number of studies have compared fat-poor AML and clear cell RCC in terms of patterns of decrease in signal intensity at chemical-shift MRI.

The number of fat-poor AMLs may influence differentiation from RCC with chemical-shift MRI [2]. If the number of fat-poor AMLs increases, this lesion tends to have a greater loss of signal intensity on opposed-phase MR images than RCC does [18, 26]. In contrast, if the number of fat-poor AMLs decreases, it is difficult to differentiate AML from RCC with chemical-shift MRI [19–22]. As a result, fat-poor AML may cause sub-

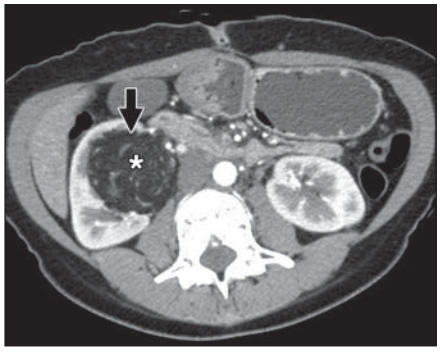

Fig. 1—37-year-old woman with fat-rich angiomyolipoma (AML). Axial contrast-enhanced CT image shows abundant fat (*asterisk*), which is main tissue in right renal fat-rich AML (*arrow*). Lesion attenuation value is –74 HU.

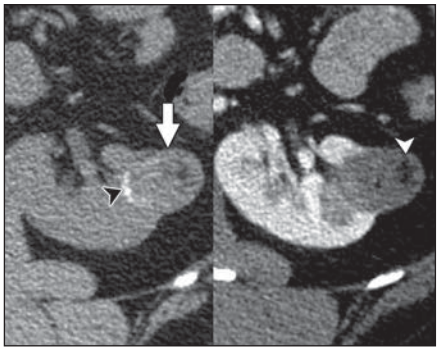

Fig. 2—50-year-old man with fat-containing renal cell carcinoma. Axial unenhanced CT image (*left*) shows curvilinear calcification (*arrowhead*) in left renal mass (*arrow*). Axial contrast-enhanced CT image (*right*) shows focal fat (*arrowhead*), which is small in relation to lesion size. Fat attenuation value is –45 HU. Percutaneous biopsy confirmed papillary renal cell carcinoma, and partial nephrectomy was performed.

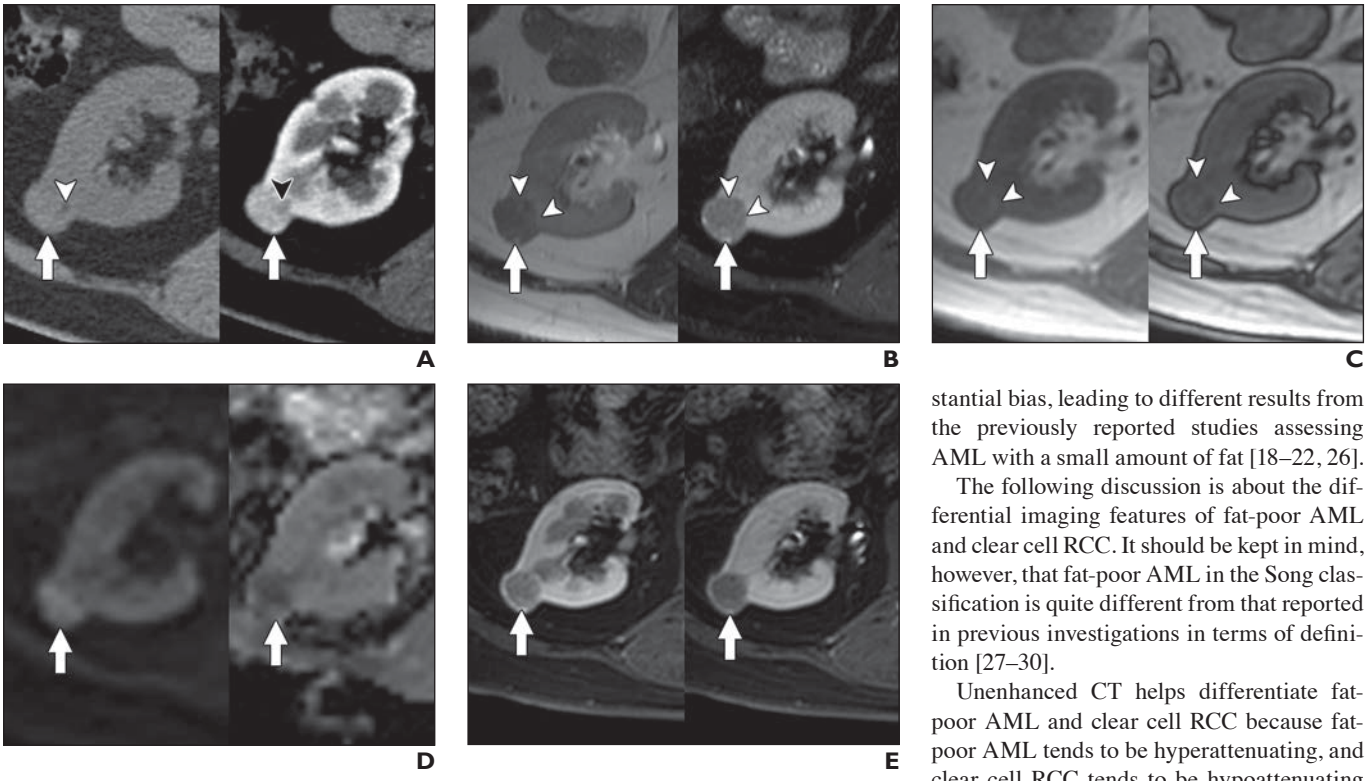

Fig. 3—56-year-old woman with fat-poor angiomyolipoma.
A, Axial unenhanced CT image (*left*) shows right renal mass (*arrow*) in which hypoattenuating area (*arrowhead*) measures –2 HU. Other hyperattenuating area measures 42 HU. Axial contrast-enhanced CT image (*right*) shows heterogeneous enhancement in lesion (*arrow*). Black arrowhead indicates hypoattenuating area, which corresponds to hypoattenuating area on unenhanced CT image.
B, Axial T2-weighted MR image (*left*) shows heterogeneously hypointense lesion (*arrow*) with two hyperintense foci (*arrowheads*). Axial fat-suppressed T2-weighted MR image (*right*) shows that lesion (*arrow*) becomes homogeneously hypointense because fat signal intensity (*arrowheads*) is suppressed.
C, Axial in-phase MR image (*left*) shows lesion (*arrow*) containing two hyperintense foci (*arrowheads*). Axial opposed-phase MR image (*right*) shows lesion (*arrow*) containing two focal areas of decreased signal intensity that correspond to hyperintense foci (*arrowheads*) on in-phase MR image.
D, Axial DW image (*left*) shows heterogeneously hyperintense lesion (*arrow*). Axial apparent diffusion coefficient map (*right*) shows heterogeneously hypointense lesion (*arrow*).
E, Axial early phase contrast-enhanced MR image (*left*) shows homogeneous enhancement of lesion (*arrow*) due to fat suppression. Axial delayed phase contrast-enhanced MR image (*right*) also shows homogeneous enhancement (*arrow*) due to fat suppression.

stantial bias, leading to different results from the previously reported studies assessing AML with a small amount of fat [18–22, 26].

The following discussion is about the differential imaging features of fat-poor AML and clear cell RCC. It should be kept in mind, however, that fat-poor AML in the Song classification is quite different from that reported in previous investigations in terms of definition [27–30].

Unenhanced CT helps differentiate fat-poor AML and clear cell RCC because fat-poor AML tends to be hyperattenuating, and clear cell RCC tends to be hypoattenuating [2, 20] (Table 2 and Figs. 3 and 4). The AML hyperattenuation results from abundant muscle, which is the main tissue in fat-poor AML [2, 24]. The RCC hypoattenuation results from abundant intracytoplasmic lipid, which is the main tissue in clear cell RCC [24, 31].

Contrast-enhanced CT is not useful for differentiating these tumors. Fat-poor AML and clear cell RCC both undergo heterogeneous enhancement [2, 32, 33] (Table 2 and Figs. 3 and 4). Fat-poor AML can exhibit various degrees of enhancement according

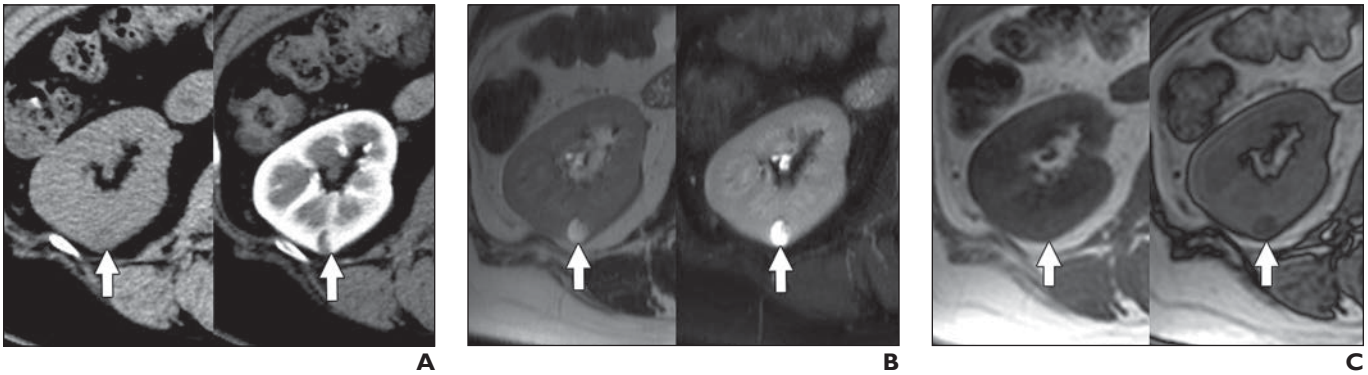

Fig. 4—65-year-old woman with clear cell renal cell carcinoma (RCC).
A, Axial unenhanced CT image (*left*) shows heterogeneously hypoattenuating mass (*arrow*) in right kidney. Lesion attenuation value is 21 HU. Axial contrast-enhanced CT image (*right*) shows heterogeneous enhancement in lesion (*arrow*).
B, Axial T2-weighted MR image (*left*) shows hyperintense lesion (*arrow*). Axial fat-suppressed T2-weighted MR image (*right*) also shows hyperintense lesion (*arrow*) without decrease in signal intensity.
C, Axial in-phase MR image (*left*) shows heterogeneously hyperintense lesion (*arrow*). Axial opposed-phase MR image (*right*) shows diffuse decrease in signal intensity in lesion (*arrow*).

(Fig. 4 continues on next page)

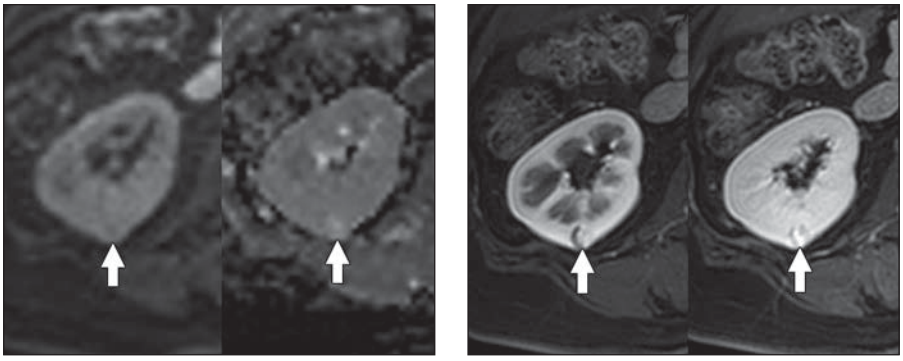

Fig. 4 (continued)—65-year-old woman with clear cell renal cell carcinoma (RCC).
D, Axial DW image (*left*) shows heterogeneously hypointense lesion (*arrow*). Axial apparent diffusion coefficient map image (*right*) shows heterogeneously hyperintense lesion (*arrow*).
E, Axial early phase contrast-enhanced MR image (*left*) shows heterogeneous lesion enhancement (*arrow*). Axial delayed phase contrast-enhanced MR image (*right*) shows slightly heterogeneous lesion enhancement (*arrow*). Ultrasound-guided biopsy confirmed that lesion was clear cell RCC.

TABLE 2: Qualitative Comparison of Fat-Poor Angiomyolipoma (AML) and Clear Cell Renal Cell Carcinoma (RCC)

CT or MRI Technique	Qualitative Imaging Features	
	Fat-Poor AML	Clear Cell RCC
Unenhanced CT	Hyperattenuating	Hypoattenuating
Contrast-enhanced CT	Heterogeneous	Heterogeneous
Chemical-shift MRI	Focal decrease in signal intensity	Diffuse decrease in signal intensity
T2-weighted MRI	Hypointense	Hyperintense
Fat-suppressed T2-weighted MRI	Hypointense	Hyperintense
Diffusion-weighted MRI	Hyperintense	Hypointense
Apparent diffusion coefficient map images	Hypointense	Hyperintense
Contrast-enhanced MRI	Heterogeneous	Heterogeneous

to the number of blood vessels. When the number of vessels decreases, the degree of enhancement is weaker than that of clear cell RCC [34, 35]. When the number of vessels increases, the degree of enhancement is similar to that of clear cell RCC [36].

T2-weighted MRI is useful for differentiating fat-poor AML from clear cell RCC. Images obtained with this MRI sequence show that fat-poor AML is hypointense and that clear cell RCC is hyperintense [2, 19, 20, 37, 38] (Table 2 and Figs. 3 and 4). The AML hypointensity also results from muscle, which is dominant in fat-poor AML [2, 19, 20, 37]. The RCC hyperintensity also results from intracytoplasmic lipid, which is abundant in clear cell RCC [19, 20, 24]. Fat-suppressed T2-weighted MRI is also useful for differentiating fat-poor AML from clear cell RCC. Fat-poor AML is more hypointense than clear cell RCC because a small amount of fat in the former is suppressed on fat-suppressed T2-weighted MR images [39].

DWI is also a useful imaging modality for differentiating fat-rich AML and clear cell RCC [2, 40, 41]. Fat-poor AML is hyperintense on DW images and has low apparent diffusion coefficient (ADC) values (Table 2 and Fig. 3) [2, 40, 41]. In contrast, clear cell RCC is hypointense on DW images and has high ADC values (Table 2 and Fig. 4) [2, 40, 41]. It is not clearly understood why these tumors have different imaging features on DW images and ADC maps. Diffusion restriction of tissue water seems to be greater in fat-poor AML than in clear cell RCC [42].

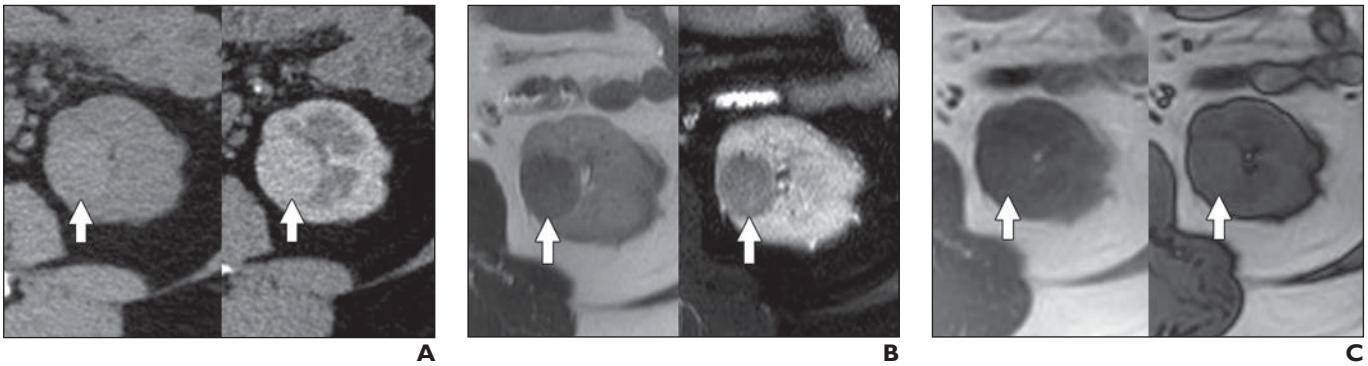

Fig. 5—49-year-old woman with fat-invisible angiomyolipoma (AML).
A, Axial unenhanced CT image (*left*) shows hyperattenuating mass (*arrow*) in left kidney. Lesion attenuation value is 45 HU. Contrast-enhanced CT image (*right*) shows homogeneously hypoattenuating lesion (*arrow*).
B, Axial T2-weighted MR image (*left*) shows homogeneously hypointense lesion (*arrow*). Fat-suppressed axial MR image (*right*) shows homogeneously hypointense lesion (*arrow*).
C, Axial in-phase MR image (*left*) shows homogeneously hyperintense lesion (*arrow*). Axial opposed-phase MR image (*right*) shows no decrease in signal intensity in lesion (*arrow*).

(Fig. 5 continues on next page)

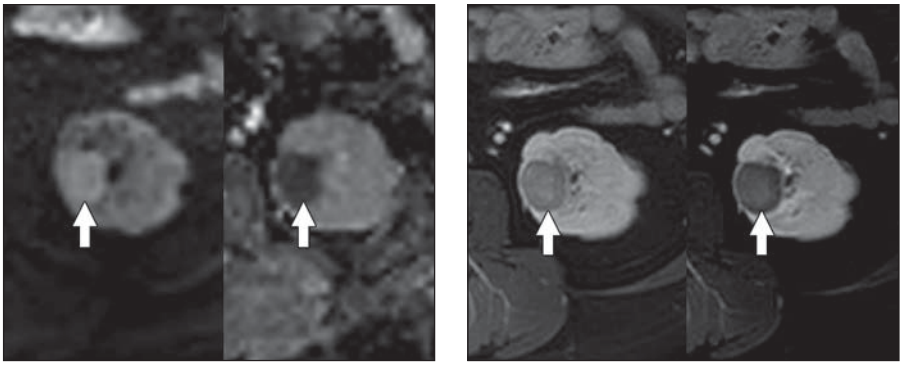

Fig. 5 (continued)—49-year-old woman with fat-invisible angiomyolipoma (AML).
D, Axial DW image (*left*) shows homogeneously hyperintense lesion (*arrow*). Axial apparent diffusion coefficient map (*right*) shows homogeneously hypointense lesion (*arrow*).
E, Axial early phase contrast-enhanced MR image (*left*) shows homogeneous lesion enhancement (*arrow*). Axial delayed phase contrast-enhanced MR image (*right*) also shows homogeneous lesion enhancement (*arrow*). Ultrasound-guided biopsy confirmed lesion was AML.

Contrast-enhanced MRI is not as useful as DWI for differentiating fat-poor AML from clear cell RCC because there is much overlap in enhancement patterns [2, 18, 43]. Both tumors exhibit heterogeneous contrast enhancement [2] (Table 2). A large number of fat-poor AMLs exhibit early wash-in and washout of contrast material, which is also a characteristic finding of clear cell RCC [18, 43]. Fat-poor AML can undergo various degrees of MRI enhancement according to the number of vessels, as in CT enhancement.

Fat-Invisible Angiomyolipoma Versus Non–Clear Cell Renal Cell Carcinoma

Fat-invisible AML is defined as a lesion measuring more than –10 HU on unenhanced CT images and having a tumor-to-spleen ratio of 0.71 or greater and a signal intensity index of 16.5% or less [1, 2] (Table 1 and Fig. 5). Many non–clear cell RCCs also have the same CT and MRI features [15, 20, 44, 45]. It is uncommon that clear cell RCC has these MRI characteristics [20]. Therefore, fat-invisible AML must be differentiated from non–clear cell RCC. Non–clear cell RCCs are defined as all histologic subtypes of RCC except clear cell RCC. These tumors include papillary, chromophobe, and other miscellaneous RCCs [20].

Qualitative analysis with a signal-intensity decrease pattern on opposed-phase MR images is not useful for differentiating fat-invisible AML from non–clear cell RCC because it is impossible to perform visual assessment of patterns of decrease in signal intensity. Neither fat-invisible AML nor non–clear cell RCC exhibits a decrease in signal intensity on opposed-phase MR images, but they both have homogeneous signal intensity on chemical-shift MR images [1, 2, 20] (Figs. 5 and 6).

Unenhanced CT shows that fat-invisible AML and non–clear cell RCC are both homogeneously hyperattenuating [2, 5, 20] (Figs. 5 and 6). Contrast-enhanced CT shows that these tumors undergo both homogeneous and persistent enhancement [2, 5, 35]. CT is not useful for differentiating fat-invisible AML and non–clear cell RCC [2, 20].

T2-weighted or fat-suppressed T2-weighted MRI shows that fat-invisible AML and non–clear cell RCC are both homogeneously hypointense [2, 3, 20, 37] (Figs. 5 and 6). DWI shows that both of these tumors exhibit strong diffusion restriction and have low ADC values [2]. Fat-invisible AML exhibits stronger diffusion restriction and has lower ADC values than fat-poor AML because it contains of more muscle and less fat [2] (Figs. 3 and 5). Contrast-enhanced MRI shows that both fat-invisible AML and non–clear cell RCC may exhibit homogeneous enhancement [2] (Figs. 5 and 6).

Angiomyolipoma Versus Renal Cell Carcinoma: Morphologic Differentiation

Lesion shape can add value to quantitative CT and MRI analysis in differentiating AML and RCC. The angular interface indicates angular configuration of the parenchymal portions of a tumor [16–18, 46, 47]. "Overflowing beer sign" indicates bulging-out portions of a tumor extending along the adjacent renal

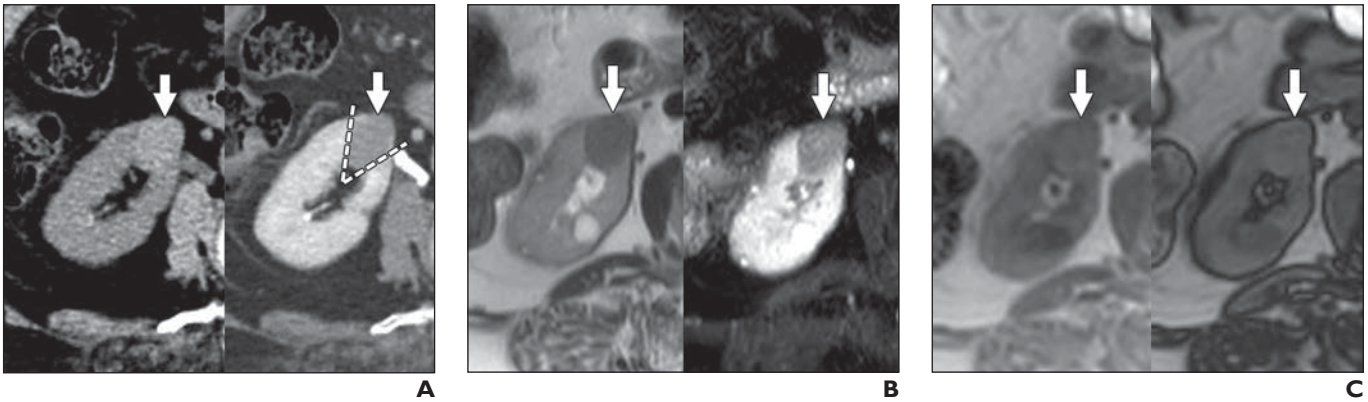

Fig. 6—69-year-old woman with papillary renal cell carcinoma (RCC).
A, Axial unenhanced CT image (*left*) shows hyperattenuating mass (*arrow*) in right kidney. Lesion attenuation value is 43 HU. Contrast-enhanced CT image (*right*) shows homogeneously hypoattenuating lesion (*arrow*) and narrow angular interface (*dashed lines*).
B, Axial T2-weighted MR image (*left*) shows homogeneously hypointense lesion (*arrow*). Axial fat-suppressed MR image (*right*) shows homogeneously hypointense lesion (*arrow*).
C, Axial in-phase MR image (*left*) shows that lesion (*arrow*) is homogeneously hyperintense. Axial opposed-phase MR image (*right*) shows no signal drop in lesion (*arrow*).

(Fig. 6 continues on next page)

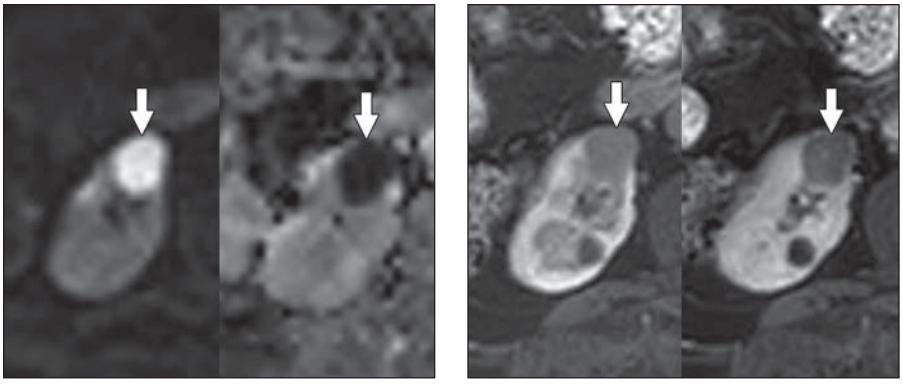

D E

Fig. 6 (continued)—69-year-old woman with papillary renal cell carcinoma (RCC).
D, Axial DW image (*left*) shows homogeneously hyperintense lesion (*arrow*). Axial apparent diffusion coefficient map (*right*) shows homogeneously hypointense lesion (*arrow*).
E, Axial early phase contrast-enhanced MR image (*left*) shows homogeneous lesion enhancement (*arrow*). Axial delayed phase contrast-enhanced MR image (*right*) also shows homogeneous lesion enhancement (*arrow*). CT-guided biopsy confirmed that lesion was papillary RCC.

surface. AML exhibits overflowing beer sign or a narrow angular interface more frequently than RCC does (Fig. 5). Many investigators [16–18, 46, 47] have reported that overflowing beer sign is more useful than narrow angular interface for differentiating AML and RCC. However, the positive predictive value of overflowing beer sign ranges from 49.3% to 68.2%, which is not enough to correctly diagnose AML. Accordingly, morphologic analysis cannot completely eliminate the necessity of biopsy. When fat-poor AML or fat-invisible AML is difficult to differentiate from RCC with quantitative CT or MRI criteria, the presence of overflowing beer sign or narrow angular interface helps to suggest AML rather than RCC. However, the absence of these morphologic features does not definitely indicate RCC, because a large number of AMLs have no overflowing beer sign or narrow angular interface (Fig. 5).

What Subtypes of Angiomyolipoma Require Biopsy?

The role of percutaneous biopsy is to avoid unnecessary surgery by means of preoperative detection of benign renal tumors [15, 44, 45, 48]. Basically, fat-rich AML does not require biopsy because the lesion is easily diagnosed with unenhanced CT alone (Table 1 and Fig. 1). In exceptional cases, however, biopsy is necessary to exclude the likelihood of fat-containing RCC when a renal mass with little fat content contains calcification or necrosis (Fig. 2).

The necessity of biopsy is still controversial, although fat-poor AML appears different from clear cell RCC on unenhanced CT, T2-weighted MR, fat-suppressed T2-weighted MR, chemical-shift MR, DW, and ADC map MR images [2, 49] (Tables 1 and 2 and Figs. 3 and 4). This is why there are only a few articles dealing with comparison of fat-poor AML and clear cell RCC [1, 2, 20]. Nevertheless, percutaneous biopsy should be performed when differentiation of these tumors is not clear at CT or MRI [2, 49]. In general, biopsy is necessary for differentiating fat-invisible AML from non–clear cell RCC because CT or MRI alone does not provide clear differentiation [15, 20, 44, 45, 48] (Table 1 and Figs. 5 and 6). The CT and MRI features of these tumors overlap considerably.

Limitations

First, a meta-analysis was not performed because of the small number of articles on the Song classification. Therefore, this review does not describe the method for choosing and analyzing published papers. It also lacks detailed analysis and significant statistics to support our argument. Second, the rationale for the importance of the recently developed Song classification of AML is somewhat lacking. Further investigation is necessary for making sound conclusions.

Conclusion

Fat-rich AML should be differentiated from fat-containing RCC if this situation is rarely encountered. A small amount of fat relative to a large tumor, calcification, or necrosis is more suggestive of RCC than of AML. In exceptional cases, biopsy is recommended if these findings are detected.

Fat-poor AML should be differentiated from clear cell RCC. This type of AML tends to be hyperattenuating on unenhanced CT images, hypointense on T2- or fat-suppressed T2-weighted MR images, hyperintense on DW images, and hypointense on ADC maps compared with clear cell RCC. Fat-poor AML is more likely than clear cell RCC to exhibit a focal decrease in signal intensity on opposed-phase MR images. The necessity of biopsy is still controversial because not enough evidence has accumulated.

Fat-invisible AML should be differentiated from non–clear cell RCC. Both tumors tend to be hyperattenuating on unenhanced CT images, negative on chemical shift MR images, hypointense on T2- or fat-suppressed T2-weighted MR images, hyperintense on DW images, and hypointense on ADC maps. Therefore, biopsy is necessary to differentiate these tumors.

CT or MRI features can provide clues for differentiating fat-rich AML from fat-containing RCC and fat-poor AML from clear cell RCC. Fat-invisible AML, however, is difficult to differentiate from non–clear cell RCC on the basis of CT or MRI features. Radiologists should not be reluctant to perform biopsy when lesion differentiation is not clear at CT or MRI.

Acknowledgment

I thank Yeon Hyeon Choe, chairman of the radiology department.

References

1. Song S, Park BK, Park JJ. New radiologic classification of renal angiomyolipomas. *Eur J Radiol* 2016; 85:1835–1842
2. Park BK. Renal angiomyolipoma: radiologic classification and imaging features according to the amount of fat. *AJR* 2017; 209:826–835
3. Jinzaki M, Silverman SG, Akita H, Nagashima Y, Mikami S, Oya M. Renal angiomyolipoma: a radiological classification and update on recent developments in diagnosis and management. *Abdom Imaging* 2014; 39:588–604
4. Simpson E, Patel U. Diagnosis of angiomyolipoma using computed tomography-region of interest < or =–10 HU or 4 adjacent pixels < or =–10 HU are recommended as the diagnostic thresholds. *Clin Radiol* 2006; 61:410–416
5. Jinzaki M, Tanimoto A, Narimatsu Y, et al. Angiomyolipoma: imaging findings in lesions with minimal fat. *Radiology* 1997; 205:497–502
6. Hélénon O, Chrétien Y, Paraf F, Melki P, Denys A, Moreau JF. Renal cell carcinoma containing fat: demonstration with CT. *Radiology* 1993; 188:429–430
7. D'Angelo PC, Gash JR, Horn AW, Klein FA. Fat

in renal cell carcinoma that lacks associated calcifications. *AJR* 2002; 178:931–932

8. Hammadeh MY, Thomas K, Philp T, Singh M. Renal cell carcinoma containing fat mimicking angiomyolipoma: demonstration with CT scan and histopathology. *Eur Radiol* 1998; 8:228–229
9. Lesavre A, Correas JM, Merran S, Grenier N, Vieillefond A, Helenon O. CT of papillary renal cell carcinomas with cholesterol necrosis mimicking angiomyolipomas. *AJR* 2003; 181:143–145
10. Richmond L, Atri M, Sherman C, Sharir S. Renal cell carcinoma containing macroscopic fat on CT mimics an angiomyolipoma due to bone metaplasia without macroscopic calcification. *Br J Radiol* 2010; 83:e179–e181
11. Strotzer M, Lehner KB, Becker K. Detection of fat in a renal cell carcinoma mimicking angiomyolipoma. *Radiology* 1993; 188:427–428
12. Castoldi MC, Dellafiore L, Renne G, Schiaffino E, Casolo F. CT demonstration of liquid intratumoral fat layering in a necrotic renal cell carcinoma. *Abdom Imaging* 1995; 20:483–485
13. Schuster TG, Ferguson MR, Baker DE, Schaldenbrand JD, Solomon MH. Papillary renal cell carcinoma containing fat without calcification mimicking angiomyolipoma on CT. *AJR* 2004; 183:1402–1404
14. Wasser EJ, Shyn PB, Riveros-Angel M, Sadow CA, Steele GS, Silverman SG. Renal cell carcinoma containing abundant non-calcified fat. *Abdom Imaging* 2013; 38:598–602
15. Silverman SG, Gan YU, Mortele KJ, Tuncali K, Cibas ES. Renal masses in the adult patient: the role of percutaneous biopsy. *Radiology* 2006; 240:6–22
16. Remzi M, Ozsoy M, Klingler HC, et al. Are small renal tumors harmless? Analysis of histopathological features according to tumors 4 cm or less in diameter. *J Urol* 2006; 176:896–899
17. Richard PO, Jewett MA, Bhatt JR, et al. Renal tumor biopsy for small renal masses: a single-center 13-year experience. *Eur Urol* 2015; 68:1007–1013
18. Sasiwimonphan K, Takahashi N, Leibovich BC, Carter RE, Atwell TD, Kawashima A. Small (<4 cm) renal mass: differentiation of angiomyolipoma without visible fat from renal cell carcinoma utilizing MR imaging. *Radiology* 2012; 263:160–168
19. Hindman N, Ngo L, Genega EM, et al. Angiomyolipoma with minimal fat: can it be differentiated from clear cell renal cell carcinoma by using standard MR techniques? *Radiology* 2012; 265:468–477
20. Jeong CJ, Park BK, Park JJ, Kim CK. Unenhanced CT and MRI parameters that can be used to reliably predict fat-invisible angiomyolipoma. *AJR* 2016; 206:340–347
21. Jhaveri KS, Elmi A, Hosseini-Nik H, et al. Predictive value of chemical-shift MRI in distinguishing clear cell renal cell carcinoma from non-clear cell renal cell carcinoma and minimal-fat angiomyolipoma. *AJR* 2015; 205:[web]W79–W86
22. Dillon RC, Friedman AC, Miller FH. MR signal intensity calculations are not reliable for differentiating renal cell carcinoma from lipid poor angiomyolipoma. *Radiology* 2010; 257:299–300
23. Outwater EK, Bhatia M, Siegelman ES, Burke MA, Mitchell DG. Lipid in renal clear cell carcinoma: detection on opposed-phase gradient-echo MR images. *Radiology* 1997; 205:103–107
24. Krishnan B, Truong LD. Renal epithelial neoplasms: the diagnostic implications of electron microscopic study in 55 cases. *Hum Pathol* 2002; 33:68–79
25. Motzer RJ, Bander NH, Nanus DM. Renal-cell carcinoma. *N Engl J Med* 1996; 335:865–875
26. Kim JK, Kim SH, Jang YJ, et al. Renal angiomyolipoma with minimal fat: differentiation from other neoplasms at double-echo chemical shift FLASH MR imaging. *Radiology* 2006; 239:174–180
27. Cardone G, D'Andrea A, Piscioli I, Scialpi M. Fat-poor angiomyolipoma and renal cell carcinoma: differentiation with MR imaging and accuracy of histopathologic evaluation. *Radiology* 2012; 265:979–980
28. Potretzke AM, Potretzke TA, Bauman TM, et al. Computed tomography and magnetic resonance findings of fat-poor angiomyolipomas. *J Endourol* 2017; 31:119–128
29. Tanaka H, Fujii Y, Tanaka H, et al. Stepwise algorithm using computed tomography and magnetic resonance imaging for diagnosis of fat-poor angiomyolipoma in small renal masses: development and external validation. *Int J Urol* 2017; 24:511–517
30. Woo S, Kim SY, Cho JY, Kim SH. Differentiation between papillary renal cell carcinoma and fat-poor angiomyolipoma: a preliminary study assessing detection of intratumoral hemorrhage with chemical shift MRI and T2*-weighted gradient echo. *Acta Radiol* 2018; 59:627–634
31. Yoshimitsu K, Honda H, Kuroiwa T, et al. MR detection of cytoplasmic fat in clear cell renal cell carcinoma utilizing chemical shift gradient-echo imaging. *J Magn Reson Imaging* 1999; 9:579–585
32. Jung SC, Cho JY, Kim SH. Subtype differentiation of small renal cell carcinomas on three-phase MDCT: usefulness of the measurement of degree and heterogeneity of enhancement. *Acta Radiol* 2012; 53:112–118
33. Kim JK, Kim TK, Ahn HJ, Kim CS, Kim KR, Cho KS. Differentiation of subtypes of renal cell carcinoma on helical CT scans. *AJR* 2002; 178:1499–1506
34. Xie P, Yang Z, Yuan Z. Lipid-poor renal angiomyolipoma: differentiation from clear cell renal cell carcinoma using wash-in and washout characteristics on contrast-enhanced computed tomography. *Oncol Lett* 2016; 11:2327–2331
35. Kim JK, Park SY, Shon JH, Cho KS. Angiomyolipoma with minimal fat: differentiation from renal cell carcinoma at biphasic helical CT. *Radiology* 2004; 230:677–684
36. Woo S, Suh CH, Cho JY, Kim SY, Kim SH. Diagnostic performance of CT for diagnosis of fat-poor angiomyolipoma in patients with renal masses: a systematic review and meta-analysis. *AJR* 2017; 209:[web]W297–W307
37. Choi HJ, Kim JK, Ahn H, Kim CS, Kim MH, Cho KS. Value of T2-weighted MR imaging in differentiating low-fat renal angiomyolipomas from other renal tumors. *Acta Radiol* 2011; 52:349–353
38. Kim Y, Sung DJ, Sim KC, et al. Renal tumors with low signal intensities on T2-weighted MR image: radiologic-pathologic correlation. *Abdom Radiol (NY)* 2017; 42:2108–2118
39. Chung MS, Choi HJ, Kim MH, Cho KS. Comparison of T2-weighted MRI with and without fat suppression for differentiating renal angiomyolipomas without visible fat from other renal tumors. *AJR* 2014; 202:765–771
40. Tanaka H, Yoshida S, Fujii Y, et al. Diffusion-weighted magnetic resonance imaging in the differentiation of angiomyolipoma with minimal fat from clear cell renal cell carcinoma. *Int J Urol* 2011; 18:727–730
41. Ding Y, Zeng M, Rao S, Chen C, Fu C, Zhou J. Comparison of biexponential and monoexponential model of diffusion-weighted imaging for distinguishing between common renal cell carcinoma and fat poor angiomyolipoma. *Korean J Radiol* 2016; 17:853–863
42. Sivrioglu AK, Aribal S, Hakan OR. Distinguishing between renal cell Carcinoma and fat poor angiomyolipoma in diffusion-weighted imaging. *Korean J Radiol* 2017; 18:410–411
43. Wang HY, Su ZH, Xu X, et al. Dynamic contrast-enhanced MRI in renal tumors: common subtype differentiation using pharmacokinetics. *Sci Rep* 2017; 7:3117
44. Silverman SG, Israel GM, Herts BR, Richie JP. Management of the incidental renal mass. *Radiology* 2008; 249:16–31
45. Sahni VA, Silverman SG. Biopsy of renal masses: when and why. *Cancer Imaging* 2009; 9:44–55
46. Pahernik S, Ziegler S, Roos F, Melchior SW, Thuroff JW. Small renal tumors: correlation of clinical and pathological features with tumor size. *J Urol* 2007; 178:414–417; discussion, 416–417
47. Kim YH, Han K, Oh YT, Jung DC, Cho NH, Park SY. Morphologic analysis with computed tomography may help differentiate fat-poor angiomyolipoma from renal cell carcinoma: a retrospective study with 602 patients. *Abdom Radiol (NY)* 2018; 43:647–654
48. Sahni VA, Silverman SG. Imaging management of incidentally detected small renal masses. *Semin Intervent Radiol* 2014; 31:9–19
49. Kufer V, Schwab SA, Buttner M, Agaimy A, Uder M, Amann K. Incidental monotypic (fat-poor) renal angiomyolipoma diagnosed by core needle biopsy. *Case Rep Med* 2012; 2012:906924